Furin-mediated release of soluble hemojuvelin: a new link between hypoxia and iron homeostasis

Laura Silvestri,[1] Alessia Pagani,[1] and Clara Camaschella[1]

[1]Vita-Salute San Raffaele University–Istituto di Ricovero e Cura a Carattere Scientifico (IRCCS), San Raffaele, Milan, Italy

The liver peptide hepcidin regulates iron absorption and recycling. Hemojuvelin (HJV) has a key role in hepcidin regulation, and its inactivation causes severe iron overload both in humans and in mice. Membrane HJV (m-HJV) acts as a coreceptor for bone morphogenetic proteins (BMPs), whereas soluble HJV (s-HJV) may down-regulate hepcidin in a competitive way interfering with BMP signaling. s-HJV is decreased by iron in vitro and increased by iron deficiency in vivo. However, the mechanisms regulating the 2 HJV isoforms remain unclear. Here we show that s-HJV originates from a furin cleavage at position 332–335. s-HJV is reduced in the cleavage mutant R335Q as well as in cells treated with a furin inhibitor, and increased in cells overexpressing exogenous furin, but not in cells overexpressing an inactive furin variant. Furin is up-regulated by iron deficiency and hypoxia in association with the stabilization of HIF-1α. Increased s-HJV in response to HIF-1α occurs during differentiation of murine muscle cells expressing endogenous Hjv. Our data are relevant to the mechanisms that relate iron metabolism to the hypoxic response. The release of s-HJV might be a tissue-specific mechanism, signaling the local iron requests of hypoxic skeletal muscles independently of the oxygen status of the liver. (Blood. 2008;111:924-931)

Introduction

The liver peptide hepcidin is the key regulator of systemic iron homeostasis[1] since it determines the level of circulating iron controlling intestinal iron absorption and macrophage iron recycling. Hemojuvelin (HJV) is a recently recognized protein that plays a crucial role in the regulation of hepcidin. The *HJV* gene, encoding HJV, is the gene of 1q-linked juvenile hemochromatosis, a recessive disease that leads to severe iron overload of early onset (hemochromatosis type 2A, OMIM no. 602390).[2] Patients with mutated *HJV* as well as $Hjv^{-/-}$ mice[3,4] have low/absent hepcidin levels, indicating that HJV modulates hepcidin. HJV is expressed in liver, skeletal muscle, and heart[2] and belongs to the family of repulsive guidance molecules (RGMs), expressed mainly in the central nervous system.[5,6] As are the other RGM proteins, HJV is characterized by a signal peptide, a RGD motif, a partial von Willebrand factor type D domain, and a glycosilphosphatidylinositol (GPI)–anchor domain.[2] HJV undergoes a partial autocatalytic cleavage[7] to reach the plasma membrane (m-HJV) as a cleaved heterodimer.[8,9]

Recently, it was shown that HJV is a coreceptor for bone morphogenetic proteins (BMPs) and that hepcidin regulation occurs via the BMP/SMAD pathway.[10,11] BMP2 and BMP4 signaling is dependent on diferric transferrin, thus establishing a link between HJV-BMP and iron.[12] HJV exists in 2 forms: a membrane-bound (m-HJV) and a soluble one (s-HJV), which in vitro reciprocally regulate hepcidin expression in response to opposite iron changes.[7] s-HJV is able to interfere with and to block the signaling of BMP2 and BMP4 both in vitro[12] and in vivo.[13]

We have previously documented the relevance of m-HJV in the molecular pathogenesis of juvenile hemochromatosis, providing evidence that at least some of the mutants identified as causal in patients are less efficiently targeted to the plasma membrane, compared with the wild-type protein.[9]

Generation of s-HJV appears to be a regulated process decreased by iron treatment and diferric transferrin.[7] During our previous study, we have confirmed that this regulation is maintained in mutants, strengthening that s-HJV, suppressed by iron overload, is not involved in the disease pathogenesis.[9] We have also suggested that s-HJV does not derive from shedding of m-HJV, since its release in the medium is observed even in mutants that barely reach the plasma membrane. The discrepancy between the presence of m-HJV and the production of s-HJV is also well exemplified by the efficient secretion of soluble forms from variants unable to reach the plasma membrane because they were truncated at the GPI addition site.[8,9] On these bases and because isolated membranes do not release s-HJV,[9] we proposed that the soluble form results from cell secretion.

In this paper, we demonstrate that s-HJV is the product of a furin cleavage at the C-terminus of the protein that occurs mainly in the endoplasmic reticulum (ER) and is up-regulated in conditions of iron deficiency/hypoxia.

Methods

Generation of wild-type and HJV variants

The whole *HJV* open reading frame was amplified from human cDNA and modified to introduce a cMYC tag, as described,[9] to obtain the pcDNA3.1-*HJV* construct (Figure 1A). To generate the *HJV* R335Q variant, pcDNA3.1-*HJV* was mutagenized using the QuickChange site-directed mutagenesis kit (Stratagene, La Jolla, CA), according to the manufacturer's protocol and

Submitted July 10, 2007; accepted October 10, 2007. Prepublished online as *Blood* First Edition paper, October 15, 2007; DOI 10.1182/blood-2007-07-100677.

The online version of this article contains a data supplement.

The publication costs of this article were defrayed in part by page charge payment. Therefore, and solely to indicate this fact, this article is hereby marked "advertisement" in accordance with 18 USC section 1734.

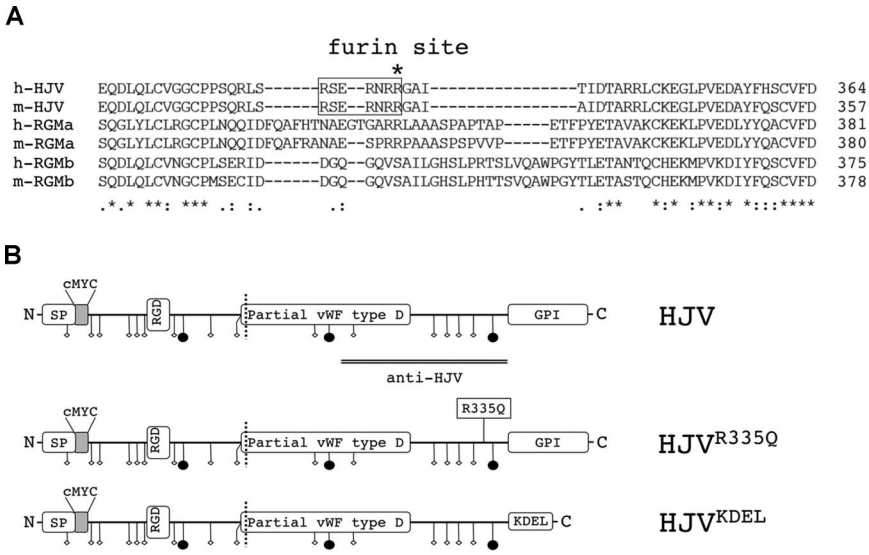

Figure 1. Scheme of constructs and sequence alignment of the regions encompassing the furin motif of RGM proteins. (A) ClustalW alignment (http://www.ebi.ac.uk/clustalw)[14] of human RGMs, showing amino acidic conservation 5′ and 3′ of the furin motif. RSER^{332}NRR^{335} consensus sequence is boxed. The * above the boxed motif marks arginine 335. The degrees of conservation between proteins are indicated as follows: * indicates identical residue; :, conserved substitution; and ., semiconserved substitution. (B) From top to bottom, schematic representation of HJV functional domains in wild-type HJV and localization of the studied mutation (HJV^{R335Q}) and chimeric variant (HJV^{KDEL}). SP indicates signal peptide; RGD, arginine-glycine–aspartic acid integrin-binding domain; ◇, Cys residue; and ●, Asn residue. The dotted line indicates the autoproteolytic site. The double line shows the peptide used for the antibody production.

using the following oligonucleotides: 5′-atcagagcgcaatcgtcagggagctataaccattg-3′ (sense); 5′-caatggttatagctccctgacgattgcgctctgat-3′ (antisense) (HJV^{R335Q}, Figure 1A). To prepare the ER-retained variant, the *HJV* cDNA (truncated by 84 nucleotides at the 3′ end) was amplified from pcDNA3.1-*HJV* to introduce the KDEL motif, an ER-retention signal,[15] instead of the GPI anchor by using the following oligonucleotides: 5′-ccc*aagctt*atgggggagccaggccagtcc-3′ (sense, *Hin*dIII tail) and 5′-gg*aattc*CTATAATTCATCTTTtgaggggaagagatgcagcttctc-3′ (antisense, *Eco*RI tail; in uppercase: KDEL plus the stop codon). The amplification product was then cloned into the *Hin*dIII and *Eco*RI sites of pcDNA3.1(+) (Invitrogen, Carlsbad, CA) to make the pcDNA3.1-*HJV*-KDEL construct (HJV^{KDEL}, Figure 1A). To introduce the W191C substitution, *HJV*-KDEL was mutagenized to obtain the W191C-KDEL construct (W191C^{KDEL}), using the QuickChange site-directed mutagenesis kit and the following oligonucleotides: 5′-gccgtgtccaaggagcttgccctctactggataatgac-3′ (sense); 5′-gtcattatccagtagagggcaagctccttggacacggc-3′ (antisense). Cloning and mutagenesis products were verified by sequencing.

Generation of furin expression vectors

The whole *FUR* open reading frame was amplified from human cDNA using the following oligonucleotides: 5′-g*gaattc*cccatggagctgaggccctggttg-3′ (sense, *Eco*RI tail) and 5′-gc*tctaga*tcagagggcgctctggtctttg-3′ (antisense, *Xba*I tail), and cloned into the *Eco*RI and *Xba*I sites of pcDNA3.1(+) (Invitrogen) to make the pcDNA3.1-*FUR* construct (furin). To generate the *FUR* W547R inactive variant,[16] pcDNA3.1-*FUR* was mutagenized using the QuickChange site-directed mutagenesis kit (Stratagene), according to the manufacturer's protocol and using the following oligonucleotides: 5′-gatccctctggcgagcgggtcctagagattg-3′ (sense); 5′-caatctctaggacccgctcgccagagggatc-3′ (antisense) (furin^{W547R}). Cloning and mutagenesis products were verified by sequencing.

Antibodies

To generate rabbit polyclonal antisera directed against HJV, the recombinant GST fusion protein (see Silvestri et al for details)[9] was produced in *E coli,* purified according to standard procedures, and used to immunize rabbits (Primm, Milan, Italy). Anti–HIF-1α and anti-furin were from Santa Cruz Biotechnology (Santa Cruz, CA); anti–α-tubulin and anti-cMYC were from Invitrogen and Novus Biological (Littleton, CO), respectively. Anti–myosin heavy chain (MyHC) was from Developmental Studies Hybridoma Bank (DSHB; University of Iowa, Iowa City).

Cell cultures and reagents

Cell-culture media and reagents were from Invitrogen and from Sigma-Aldrich (St Louis, MO). HeLa and HepG2 cells were cultured in Dulbecco modified Eagle medium (DMEM) supplemented with 2 mM L-glutamine, 200 U/mL penicillin, 200 mg/mL streptomycin, 1 mM sodium pyruvate, and 10% heat-inactivated fetal bovine serum (FBS) at 37°C in 95% humidifier air and 5% CO_2. The C2C12 mouse myoblast cell line was cultured in DMEM 10% FBS under standard conditions. To generate myotubes, 80% confluent cells were shifted to differentiation medium (DMEM supplemented with 2% horse serum) and were maintained for 3 days. Differentiation was determined by morphologic changes and by the myosin heavy chain (MyHC) induction.

Western blot analysis

Cells were seeded in 100-mm–diameter dishes until 70% to 80% of confluence was reached. HeLa and HepG2 were transfected with 20 μg plasmid DNA and 50 μL Lipofectamine 2000 (Invitrogen), according to the manufacturer's instructions. After 18 hours the medium was replaced; cells were collected after 24 hours and lysed in radioimmunoprecipitation assay (RIPA) buffer.

Proteins were quantified using the Bio-Rad Protein Assay (Bio-Rad, Hercules, CA); samples (50 μg) were subjected to 10% sodium dodecyl sulfate–polyacrylamide gel electrophoresis (SDS-PAGE) and transferred to Hybond C membrane (Amersham Biosciences Europe, Freiburg, Germany) by standard Western blotting technique. Blots were incubated with the primary antisera at dilutions recommended by the manufacturer. Anti-HJV and anti–α-tubulin were used at 1:1000. Anti–HIF-1α and anti-furin were used at 1:200. After washing with TBS (0.5 M Tris-HCl [pH 7.4] and 0.15 M NaCl) containing 0.1% Tween-20, blots were incubated with relevant HRP-conjugated secondary antisera and developed using a chemiluminescence detection kit (enhanced chemiluminescence [ECL]; Amersham Biosciences Europe).

Analysis of soluble HJV

HeLa and HepG2 were transiently transfected as described in "Western blot analysis" and media replaced after 18 hours. Both transfected cells and murine myoblasts/myotubes were incubated with serum-free media, which were collected, concentrated using 5 kDa molecular weight (MW) cutoff ultrafiltration (Amicon Ultra; Millipore, Billerica, MA), and analyzed by SDS-PAGE. When indicated, 300 μM of the iron-chelator deferoxamine (DFO), 100 μM of the iron donor ferric ammonium citrate (FAC) plus 200 μM of ascorbate, 50 μM of the furin inhibitor decanoyl-Arg-Val-Lys-Arg-chloromethylketone (CMK; Alexis Biochemicals, San Diego, CA), or 500 μM cobalt chloride ($CoCl_2$) was added to the cell culture.

For the analysis of furin overexpression, HeLa cells were transiently transfected with *HJV* cDNA in the presence of *FUR* cDNA (furin) or *FUR* W547R (furin^{W547R}) variant. The total amount of DNA was maintained by

cotransfection with the empty vector pcDNA3.1. Cells and media were then processed and analyzed.

Luciferase assay for furin promoter activity

HeLa cells were transiently transfected with Lipofectamine 2000 using the *FUR* promoter construct, pGL2-P1 (generously provided by Prof Claire Dubois, Immunology and Pulmonary Division, Faculty of Medicine, University of Sherbrooke, Sherbrooke, QC),[17] or the empty vector pGL2, together with the pRL-CMV vector, which was used as an internal control of transfections. After 12 hours, cells were incubated in serum-free media in the presence of $CoCl_2$ (500 μM), DFO (300-600 μM), and FAC (100-300 μM plus 200 μM of ascorbate) for 6 hours. Cells were then lysed and analyzed for luciferase expression using the Dual Luciferase Reportes assay (Promega, Milan, Italy), according to the manufacturer's instructions. Values were normalized for transfection efficiency. The Student *t* test was used for statistical calculation.

Cell surface expression of HJV

Quantification of cell surface expression of HJV was performed as described,[9] with minor modifications. In brief, 10^4 HeLa or HepG2 cells were seeded in 48-well plates and transfected with 0.4 μg plasmid DNA complexed with 1 μL Lipofectamine 2000, according to the manufacturer's instructions. After 12 hours, the medium was replaced, and 24 hours later cells were fixed with 4% paraformaldehyde for 45 minutes at room temperature. Cells were washed with PBS, blocked with 5% nonfat milk in PBS, incubated with anti-HJV (1:1000) and then with the relative secondary HRP antibody, at 37°C. Since the rabbit anti-HJV antibody was not previously used for this purpose, the antibody was first tested in immunofluorescence (Figure S1, available on the *Blood* website; see the Supplemental Materials link at the top of the online article). For total HJV expression, cells were permeabilized with 0.1% Triton X-100 in PBS, prior to blocking and incubation with anti-HJV. Peroxidase activity was measured with an HSR substrate (o-phenylenediamine dihydrochloride), according to the manufacturer's instructions. The amount of m-HJV was calculated as the ratio between the absorbance of unpermeabilized and permeabilized cells. Background absorbance was subtracted for each sample. The Student *t* test was used for statistical calculation.

EM and morphometric analysis

HeLa cells were transiently transfected with Lipofectamine 2000 using pcDNA3.1-*HJV* (HJV) and pcDNA-*HJV*KDEL (HJV^{KDEL}) constructs. After 18 hours, cells were fixed, labeled with a polyclonal goat anti-MYC using the gold-enhance protocol, embedded in Epon-812, and cut as described.[18] Immunoelectron microscopy (EM) images were acquired from thin sections under a Philips Tecnai-12 electron microscope (Philips, Eindhoven, the Netherlands) using an ULTRA VIEW CCD digital camera (Philips). Thin sections were also used to quantify gold particles residing within different compartments of the secretory pathway.

Results

A specific furin cleavage site of HJV

In the hypothesis that the mechanism generating s-HJV is a proteolytic event at the C-terminal part of the protein, we analyzed the HJV sequence using different bioinformatic approaches to search for protease-specific moieties. ELM (http://elm.eu.org)[19] and ProP 1.0 (http://www.cbs.dtu.dk)[20] algorithms predicted the existence of a furin consensus cleavage site ($R^{332}NRR^{335}\downarrow$) at position 335, which is conserved among human, mouse (Figure 1A), and rat. The furin cleavage site is present also in zebrafish HJV, although at different position. The motif is absent in RGMa and RGMb (Figure 1A), the 2 proteins highly homologous to HJV. Interestingly, RGMa and RGMb do not release a soluble protein, and indeed the algorithms do not identify a furin consensus sequence, suggesting that the furin motif is characteristic of HJV. The same site was recently identified by a different approach by Lin et al.[21]

Furin is responsible for soluble HJV production

To understand whether the furin consensus cleavage site is involved in the generation of s-HJV, we mutagenized the *HJV* cDNA, changing arginine 335 to glutamine (Figure 1B). The amino acidic substitution abrogates the furin consensus sequence recognized by ELM and ProP 1.0 algorithms. In addition, HeLa cells, transfected with the wild-type form of *HJV,* were treated with decanoyl-Arg-Val-Lys-Arg-chloromethylketone (CMK) to inhibit the endogenous furin activity, and cell culture supernatants were concentrated and analyzed using anti-HJV. This antibody recognizes 2 species: a major one of approximately 42 kDa and a minor one of approximately 33 kDa.[9] The 42-kDa species migrates as a doublet (Figure 2A) due to different glycosylation, as demonstrated by the peptide N-glycosidase F treatment (data not shown). Cells transfected with HJV^{R335Q} or treated with CMK showed a similar dramatic reduction of s-HJV. The HJV autoproteolytic processing was not impaired in R335Q variant, or CMK-treated cells, as demonstrated by the presence of the 33-kDa band in the total lysates (Figure 2A arrow), and also the plasma membrane presentation was similarly maintained (Figure 2B). These observations were successfully replicated in HepG2, confirming that furin cleavage is a common mechanism for the generation of s-HJV (Figure 2C). From these results, we conclude that both the integrity of the furin consensus cleavage site of HJV and the activity of the endogenous furin are necessary to release s-HJV. Overexpression of *FUR* cDNA in the presence of HJV strongly increased the amount of soluble species (both 42 and 33 kDa) released in the media and recognized by anti-HJV. The relevance of the endogenous furin activity is strengthened by the decrease of s-HJV when the inactive furin variant W547R[16] was overexpressed (Figure 2D).

Iron and hypoxia control s-HJV production through the modulation of furin

It has been previously shown that iron overload reduces s-HJV production.[7,9] Since furin is responsible for the proteolytic event that causes s-HJV release, we hypothesized that the furin level is modulated by iron. To this aim, transiently transfected cells were incubated for 8 hours in serum-free media, in the presence of the iron chelator deferoxamine (DFO). At this time point, DFO does not induce apoptosis in HeLa cells (Figure S2). The treatment induces iron depletion, as shown by the decreased levels of endogenous ferritin H (FTH) (Figure S3A) and stimulates s-HJV production in HeLa (Figure 3A). In the presence of DFO, furin increases (Figure 3A), suggesting that the augmented s-HJV level is due to the proconvertase up-regulation. It has been recently shown that furin is induced by hypoxia-inducible factor-1α (HIF-1α)[17] and that HIF-1α is stabilized by hypoxia and iron depletion.[22,23] During DFO treatment, the HIF-1α level increases and the *FUR* promoter is activated in a concentration-dependent manner (Figure 3A), indicating that the DFO-treated cells modulate s-HJV production through the stabilization of HIF-1α and the consequent induction of furin. The s-HJV increase by DFO was demonstrated also in HepG2 cells (Figure S4).

To further prove that the DFO-dependent s-HJV production is related to the HIF-1α–furin pathway, we treated cells with both DFO, to stabilize HIF-1α, and CMK, to inhibit furin activity. As shown in Figure 3B, CMK blocks s-HJV release, even in the

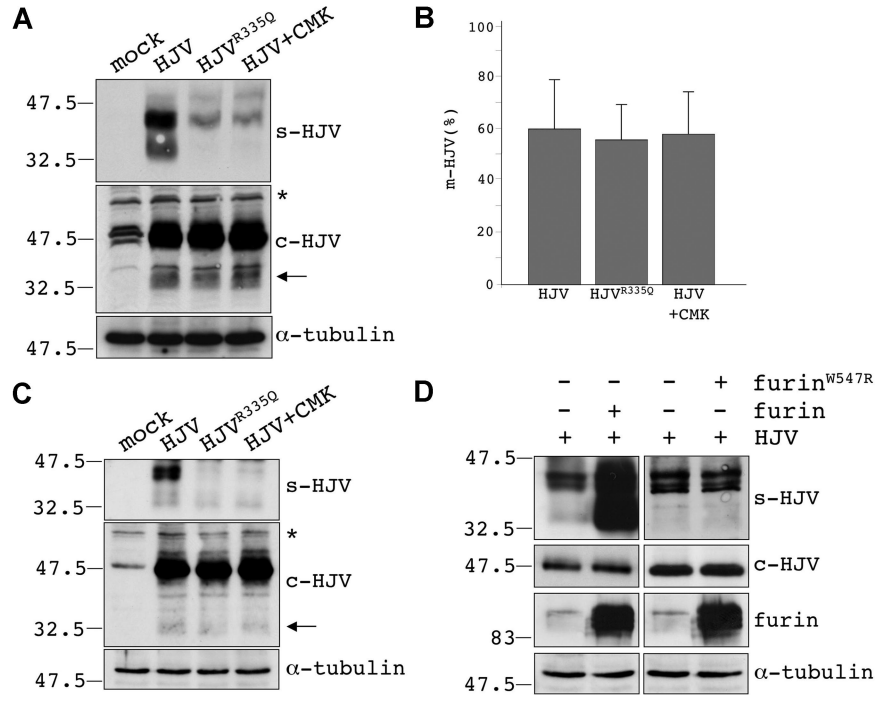

Figure 2. Furin is essential for soluble HJV production. (A) HeLa cells were transfected with empty vector (mock), wild type (HJV), and R335Q variant (HJV^{R335Q}); HJV-transfected cells were treated with 50 μM CMK to inhibit endogenous furin (HJV + CMK). After incubation for 24 hours in serum-free media, media and total lysates (50 μg) were loaded on a 10% SDS-PAGE, blotted, and analyzed by Western blot using the anti-HJV. Anti–α-tubulin was used to verify equal loading. (B) Transfected HeLa cells were fixed and incubated with anti-HJV. The amount of HJV expressed at the cell surface (unpermeabilized cells) is shown as a fraction (percentage) of total protein expression (permeabilized cells) and is indicated as m-HJV (%). Experiments were performed 3 times and made in triplicate. Error bars indicate SD. (C) Transfected HepG2 cells were treated as described in panel A, and media and total lysates were analyzed by Western blot using anti-HJV and anti–α-tubulin. (D) HeLa cells were transiently cotransfected with HJV and furin vectors, both the wild-type (furin) and the inactive variant W547R (furin^{W547R}). Media and total lysates were analyzed by Western blot using anti-HJV and anti-furin antibodies. s-HJV indicates soluble HJV; c-HJV, cell-associated HJV. The equal loading was verified by α-tubulin. CMK indicates decanoyl-Arg-Val-Lys-Arg-chloromethylketone. Arrows indicate autoproteolytically generated forms; *, unspecific bands. A further aspecific band is recognized by the anti-HJV antibody at approximately 47.5 kDa, as shown in mock lanes. Scales refer to relative molecular mass in kilodaltons.

presence of DFO, providing evidence that HIF-1α stabilization is an event upstream of furin activation and that both HIF-1α and furin are necessary for s-HJV secretion.

The regulatory mechanism linking HIF-1α and furin regulation to s-HJV production was tested during hypoxia. Transfected cells were treated for 24 hours with the chemical hypoxia inducer cobalt chloride ($CoCl_2$). The induction of hypoxia was demonstrated by the increase in HIF-1α level (Figure S5), and the lowest effective $CoCl_2$ concentration was used for functional analyses. As shown in Figure 3C, after $CoCl_2$ incubation, both s-HJV and furin protein levels are up-regulated, and the *FUR* promoter activity is increased. The effect is mediated by the HIF-1α stabilization and is not due to changes in the intracellular iron concentration, as shown by the unmodified levels of FTH (Figure S3B).

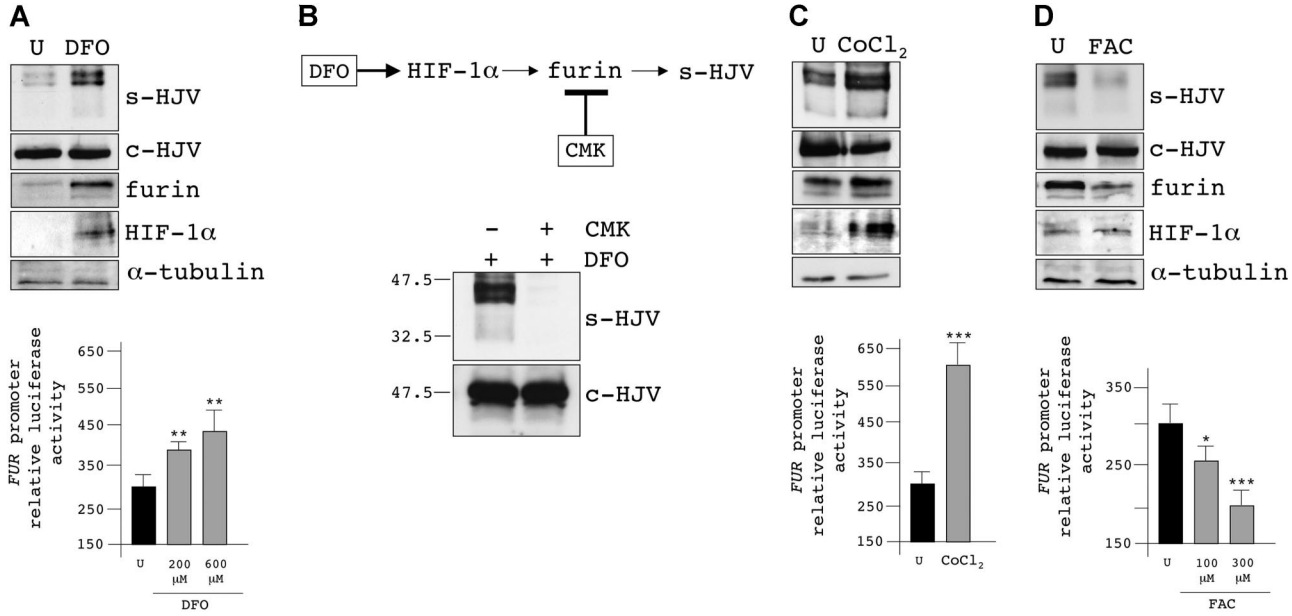

Figure 3. Iron deficiency, hypoxia, and iron overload control soluble HJV production through the regulation of furin. (A) Transfected HeLa cells were incubated for 8 hours in serum-free media in the presence of 300 μM DFO. Total lysates and concentrated media (50 μg) were analyzed using anti-HJV, anti-furin, and anti–HIF-1α. α-Tubulin was used to verify equal loading. The histogram indicates the *FUR* promoter activity, expressed as a fold induction of the luciferase reporter gene normalized on the empty vector. The Renilla activity was used to verify the transfection efficiency. Experiments were replicated 3 times. (B, top panel) Scheme of the experiment shown in the bottom panel. (B, bottom panel) Cells were treated with DFO, to activate HIF-1α, in the presence (+) or absence (−) of 50 μM CMK, to inhibit furin. Total lysates and concentrated media (50 μg) were analyzed by Western blot, using anti-HJV. The relative molecular mass, in kilodaltons, is indicated on the left. (C,D) Transfected cells were treated with 500 μM $CoCl_2$ (C) or 100 μM FAC (D) for 24 hours and analyzed as indicated in panel A. U indicates untreated; DFO, deferoxamine; $CoCl_2$, cobalt chloride; FAC, ferric ammonium citrate; s-HJV, soluble HJV; c-HJV, cell-associated HJV; and CMK, decanoyl-Arg-Val-Lys-Arg-chloromethylketone. Error bars indicate SD. *$P < .01$. **$P < .005$. ***$P < .001$.

In contrast to that observed in iron deficiency and hypoxia, iron (FAC) addition for 24 hours induces increased FTH concentration (Figure S3C) and strongly down-regulates s-HJV and furin protein levels. Accordingly, the *FUR* promoter activity decreases in a dose-dependent fashion, whereas no changes in the HIF-1α levels are observed (Figure 3C).

Modulation of soluble HJV production in muscle cells

HJV is highly expressed in the liver, heart, and skeletal muscle. Endogenous production of HJV has been demonstrated to be a sustained event during skeletal muscle differentiation in culture.[8] We differentiated murine C2C12 myoblasts and analyzed the induction of endogenous Hjv and its release in the culture media. After 72 hours of growth in differentiation medium, myoblasts morphologically change to myotubes (Figure 4A) and express the myosin heavy chain (Figure 4B). In addition, differentiated cells show high levels of both soluble and cell-associated Hjv, furin, and Hif-1α (Figure 4B). To detect Hjv, we used the same antibody raised against the human protein, which also recognizes the mouse counterpart. The protein is present in the myotube cellular lysates as a band of approximately 45 kDa, corresponding to the cell-associated murine Hjv, and in the culture media as a doublet at approximately 40 kDa, corresponding to s-Hjv. Addition of DFO had no significant effect on s-Hjv, furin, and Hif-1α protein levels (data not shown), likely because of their high basal level of expression. We conclude that even in cells expressing endogenous Hjv, the production of s-Hjv is consistent with the increased Hif-1α and furin levels.

Cleavage of HJV by furin takes place in the ER

Some plasma membrane defective HJV mutants, highly retained in the ER, produce large amounts of the 42-kDa s-HJV,[9] raising the possibility that it originates from an intracellular proteolytic activity. To demonstrate that this s-HJV species is produced by an intracellular furin, we generated a chimeric *HJV* variant, substituting a KDEL sequence (which is a well-characterized ER/early Golgi-retention signal)[15] to the natural GPI-anchor motif (Figure 1B). The HJV^{KDEL} protein does not reach the plasma membrane (Figure 5A), as demonstrated by the binding assay, and is highly retained into the ER, as shown by the EM and morphometric analysis (Figure 5B-C). The subcellular localization of the HJV^{KDEL} resembles that observed for the ER-retained HJV mutants.[9] The chimeric variant conserved the ability to release its soluble 42-kDa form in the culture media (Figure 5D). The efficiency of s-HJV production from HJV^{KDEL} was slightly reduced compared with the wild type, and other bands of lower molecular weight were released (data not shown), suggesting that the proper processing of HJV may be altered when it is artificially retained into a nonnatural compartment. Nevertheless, in the presence of CMK, the 42-kDa s-HJV from HJV^{KDEL} was undetectable, confirming that this species is generated through a furin-dependent mechanism. Since HJV^{KDEL} is almost completely retained into the ER, we conclude that the furin-dependent cleavage of HJV to produce the 42-kDa soluble form occurs mainly in this intracellular subcompartment.

Autoproteolysis occurs in the ER

HJV is processed by autoproteolysis at the Asp-Pro site at position 172[7,24] giving origin to a 33-kDa protein. This mechanism is activated at acidic pH, likely in the late secretory pathway.[9,24] However, when we analyzed the cell-associated HJV^{KDEL}, in addition to the full length we observed a cleaved band of approximately 30 kDa (Figure 5E), which was absent in the autoproteolytically defective variant W191C^{KDEL}, suggesting that also the autoproteolytic processing occurs in the ER. Interestingly, the 30-kDa species from HJV^{KDEL} migrates as a sharp band, whereas the autoproteolytic species from wild-type HJV (Figure 2A) migrates as a broad band, likely because of a complex glycosylated status due to the Golgi maturation of the wild-type proteolytic species.

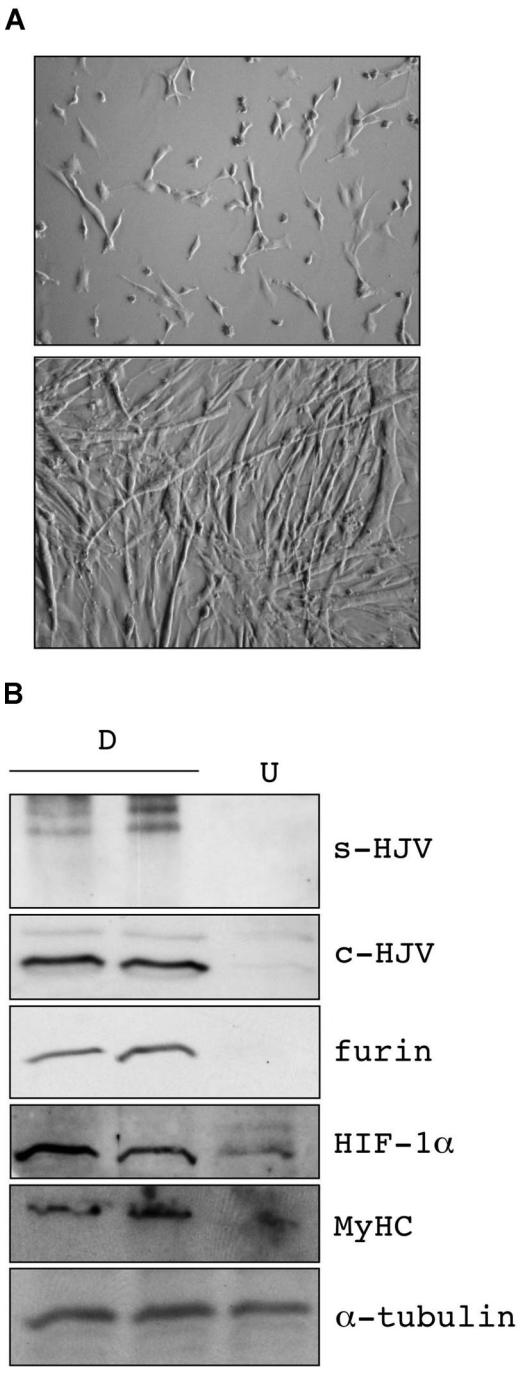

Figure 4. Modulation of soluble HJV production in differentiated murine myoblasts. (A) Morphologic differentiation of murine myoblasts (top panel) to myotubes (bottom panel) after incubation in differentiation medium for 72 hours. Phase-contrast microscopy was performed with a Leica DM IRB microscope, 20×/0.30 NA objective, and images were acquired with a Leica DC 300 FX camera and Leica IM50 software (Leica Microsystems, Wetzlar, Germany). (B) After incubation in serum-free media, media and total lysates from undifferentiated (U) and differentiated (D) cells were loaded onto a 10% SDS-PAGE, blotted, and analyzed by anti-HJV, anti-furin, anti–HIF-1α, and anti–myosin heavy chain (MyHC). α-Tubulin was used to verify equal loading.

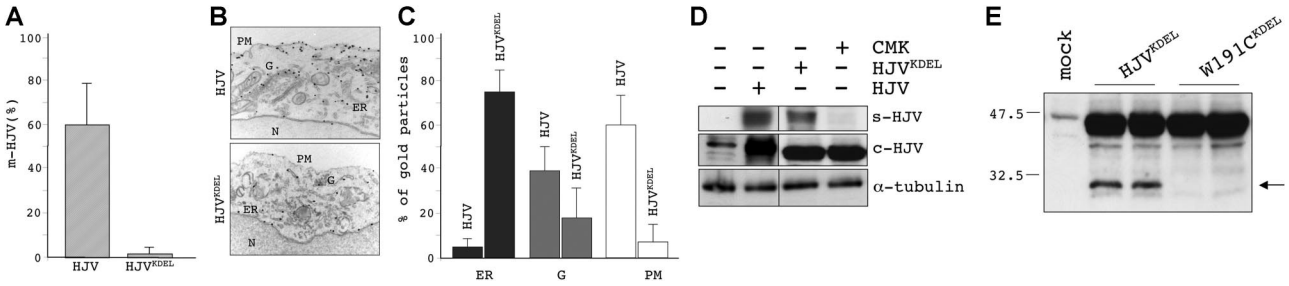

Figure 5. The furin cleavage of 42-kDa soluble HJV occurs in the ER. (A) Plasma membrane localization of wild-type HJV and HJV^{KDEL} was quantified using the described binding assay. Experiments were replicated 3 times. Error bars indicate SD. (B) HeLa cells were transiently transfected with mammalian vector encoding the wild-type HJV and HJV^{KDEL}. Eighteen hours after transfection, sections were stained with anti-cMYC using nanogold protocol as described in "EM and morphometric analysis." Images were acquired using AnalySIS software (Soft Imaging System, Lakewood, CO). Original magnification, × 23 000. PM indicates plasma membrane; ER, endoplasmic reticulum; G, Golgi; and N, nucleus. (C) Morphometric analysis of wild-type HJV and HJV^{KDEL} proteins showing the different distribution of the molecules in intracellular compartments. Black bars indicate endoplasmic reticulum (ER); gray bars, Golgi apparatus (G); and white bars, plasma membrane (PM). Error bars indicate SD. (D) Media and total lysates from cells transfected with empty vector (first lane), wild-type HJV (second lane), HJV^{KDEL} (third lane), and HJV^{KDEL} plus 50 μM CMK (fourth lane) were analyzed by Western blot and anti-HJV. Anti–α-tubulin was used to verify equal loading. s-HJV indicates soluble HJV; c-HJV, cell-associated HJV; and CMK, decanoyl-Arg-Val-Lys-Arg-chloromethylketone. (E) HeLa cells were transfected with the empty vector (mock), HJV^{KDEL}, and the autoproteolytically defective variant W191C ^{KDEL}; total lysates (50 μg) were loaded on a 10% SDS-PAGE, blotted, and analyzed using anti-HJV. The arrow indicates the autoproteolytically generated fragment. The relative molecular mass, in kilodaltons, is indicated on the left.

Discussion

Several missense mutations affecting conserved residues of the HJV protein have been described in juvenile hemochromatosis.[2,25] To further characterize the conserved motifs important for the protein function, we analyzed the protein sequence using different algorithms. Interestingly, this search identified a proprotein convertase furin cleavage site, RNRR, at positions 332-335. The same site was recently reported and the purified soluble protein originating from this cleavage characterized by mass spectrometry.[21] Comparison of the HJV sequence in the evolution revealed that the motif is highly conserved, being invariable in human, mouse, rat, and zebrafish. Although the 5′ and 3′ regions encompassing the furin cleavage motif show a high degree of conservation between all RGMs, the furin motif is not present in RGMa and RGMb, which are not characterized by the production of soluble proteins. This finding was of potential interest for HJV maturation and processing. The size of the protein expected to derive from the furin cleavage is approximately 42 kDa, compatible with the size of the glycosylated s-HJV released by cultured cells,[7,9] raising the possibility that furin is implicated in its production. To confirm this hypothesis, we first mutagenized the cleavage site of HJV changing arginine 335 to glutamine, next we studied cells treated with a furin-specific inhibitor, and finally we analyzed HJV production after cotransfection of *FUR* and *HJV*. The R335Q mutant, transiently expressed in HeLa and HepG2 cells, was cleaved at the autoproteolytic site and fully targeted to the plasma membrane, but its ability to generate s-HJV was severely hampered. Treating the same cells transfected with wild-type *HJV* with the furin inhibitor caused a drastic reduction of s-HJV production, comparable with the trace amounts released by the cleavage mutant R335Q. Cotransfection of *FUR* and *HJV* resulted in the release of very large amounts of s-HJV species of both 42 and 33 kDa. All these results demonstrate the essential role of furin in producing s-HJV. The crucial role of furin is further confirmed by the overexpression of the inactive furin variant W547R,[16] which significantly reduced s-HJV release.

Since the production of s-HJV is increased in vivo during iron deficiency,[26] we analyzed the furin expression after modulation of cellular iron status. As previously reported, iron addition suppressed s-HJV production,[7,9] but reduced also the amount of furin protein. On the contrary, iron depletion increased both s-HJV and furin. These effects were due to a modulation of the *FUR* promoter activity during changes of the intracellular iron concentration. We cannot exclude that iron directly controls furin RNA level, but we were unable to identify canonical iron-responsive elements (IREs) in *FUR* RNA UTR (data not shown). Furin promoter possesses hypoxia-responsive elements (HREs) binding sites for hypoxia-inducible factor-1 (HIF-1) transcription complex, and the levels of *FUR* mRNA are remarkably increased by hypoxia.[17] The enzyme propyl hydroxylase, which targets the subunit HIF-1α to ubiquitination and proteasome degradation, is iron dependent: for this reason, iron chelation results in HIF-1α stabilization.[27] Since HIF-1α is increased by DFO and $CoCl_2$ treatments, we conclude that in our experimental model both iron deficiency and hypoxia modulate furin via HIF-1α. The furin down-regulation observed in iron overload without evident changes of HIF-1α levels suggests the existence of other regulatory mechanisms.

Activation of s-HJV through HIF-1α is in agreement with the increased s-HJV observed during the differentiation of murine myoblasts to myotubes. Indeed, it has been reported that HIF-1α increases during muscle cell differentiation.[28] The HIF-furin–induced s-HJV release, observed in transfected cells, might be a physiologic mechanism that takes place in cells expressing endogenous HJV. Differentiating muscle cells require iron for the synthesis of myoglobin, which is estimated to contain approximately 10% to 15% of the total body iron and is an important tool for oxygen storage and release.[29,30] Increased HIF-1α has been reported during strenuous physical activity.[31,32] The release of s-HJV to suppress hepcidin could be a signal to meet the increased iron requests for myoglobin synthesis, during both differentiation and hypoxia caused by physical activity[29,30] in order to preserve muscle oxygen homeostasis.

The cellular origin of s-HJV remains controversial. It is possible that some s-HJV is shedded from m-HJV[8,21] as a 33-kDa band, since we observed this species in culture media of cells expressing wild-type HJV and membrane-competent mutants, but not in variants unable to reach the plasma membrane.[9] Moreover, we observed a relevant increase of the 33-kDa species after furin overexpression. Although we cannot exclude that this occurs in vivo, in our cellular model 42-kDa s-HJV formation is not membrane dependent. Some ER-retained HJV mutants release the

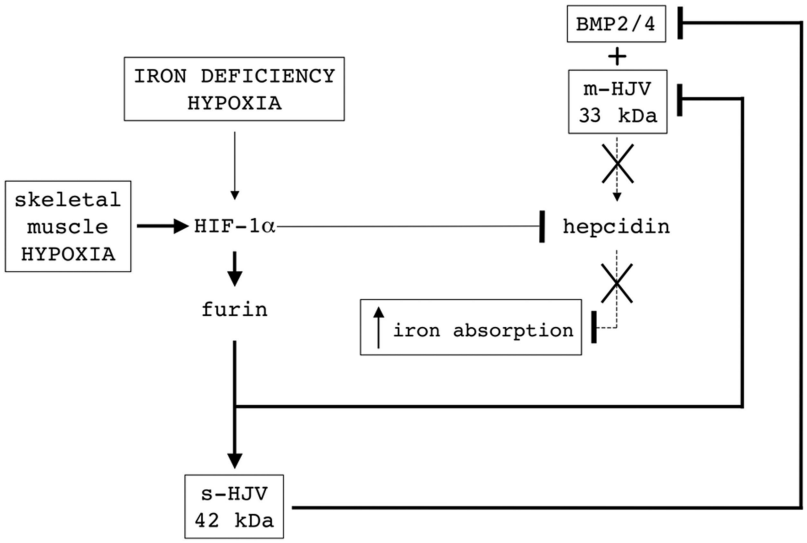

Figure 6. Scheme of iron homeostasis and hepcidin regulation in hypoxia. Systemic hypoxia/iron deficiency stabilizes HIF-1α, which may activate/inhibit the HIF-1α target genes. Among these, furin is up-regulated, while hepcidin is down-regulated. The inhibition of hepcidin increases iron absorption. Up-regulation of furin via HIF-1α may occur in hypoxic skeletal muscles (bold line) and increase s-HJV production. s-HJV, sequestering BMP2/4, blocks hepcidin activation mediated by the m-HJV/BMPs complex (dotted line) in the hepatocytes. At the same time, furin may cleave m-HJV to reduce the BMP coreceptor.

42-kDa s-HJV, suggesting that furin cleavage occurs intracellularly.[9] Similarly, HJV^{KDEL}, artificially retained in the ER, produces the 42-kDa s-HJV, which is suppressed by treatment with the furin inhibitor CMK. Thus, the furin cleavage of HJV appears to start in this cellular compartment,[33] where also the autoproteolytic process seems to take place.

Among the mutants that cause juvenile hemochromatosis, the G320V variant is highly affected in the ability to produce s-HJV,[9] likely because the substituted amino acid interferes with the close furin cleavage site. A single substitution (R335Q) expected to abrogate the furin cleavage consensus sequence has been identified at the heterozygous state in 2 HFE C282Y homozygous siblings of opposite sex with iron overload, during a search for genetic modifiers of C282Y homozygous phenotype.[34] It is unlikely that R335Q contributes to the severity of iron overload. First, the R335Q allele is expected to decrease the amount of s-HJV without interfering with the membrane export of the mutant. Second, a reduction of s-HJV should increase hepcidin activation and thus in principle it should decrease iron overload, resulting in a protective rather than worsening effect on iron overload! Unfortunately, the family segregation of the mutation was not available and the effect of the variant remains speculative.

Our data outline a model of iron regulation of hepcidin through HJV, which agrees with and completes the model recently proposed.[35] In basal conditions, HJV, as a cleaved heterodimer, reaches the plasma membrane and acts as a BMP coreceptor to activate hepcidin, when diferric transferrin increases.[12] Hypoxia directly[17] and iron deficiency indirectly (by stabilizing HIF-1α)[22,23] activate furin to release s-HJV, in order to interfere with BMP signaling and to inhibit hepcidin activation.[10,12,13] At cell surface, furin activation would rapidly reduce the amount of m-HJV, shedding the 33-kDa form, whereas intracellular furin would increase 42-kDa s-HJV with inhibitory effect on hepcidin production.[10,12] These events may occur in the same cells (hepatocytes) that produce hepcidin in order to suppress hepcidin up-regulation by an autocrine mechanism. Since HIF-1α, increased by hypoxia in the liver, can directly switch off hepcidin transcription,[35] the s-HJV local effect seems to be a redundant mechanism. However, s-HJV is released not only by the hepatocytes but also by muscle cells[8,26] (and present paper). HIF-1α might increase locally in skeletal muscles (eg, after an strenuous physical activity),[32] as an adaptive mechanism to hypoxia to signal iron needs through s-HJV. This would interrupt the BMP signaling and switch off hepcidin activation[13] in a normoxic liver. A schematic representation of the events related to hepcidin regulation by hypoxia is outlined in Figure 6. Signaling through s-HJV could represent an example of tissue-specific iron regulation, which is likely a transient mechanism before the activation of more complex adaptive mechanisms to hypoxia. This hypothesis could be directly tested in vivo.

Our data are relevant to the problem of systemic iron homeostasis and to the general mechanisms that relate hypoxia to iron metabolism.

Acknowledgments

We gratefully acknowledge Prof Claire Dubois for the pGL2-P1 *FUR* promoter construct. We are indebted to Sonia Levi and Paolo Arosio for the ferritin H reagents and critical comments on the paper, and to Paolo Arosio for the gift of the anti-HJV antibody. We also thank Roman Polishchuk from the Telethon Electron Microscopy Core Facility (TeEMCoF; Consorzio Mario Negri Sud-Santa Maria Imbaro) for the Immuno EM and morphometric analysis; Paola Picozzi for support in C2C12 growth and differentiation; and Maurilio Sampaolesi for the gift of the anti-MyHC.

This work was supported in part by Telethon Rome grant GGP05024 and EEc Framework 6 (LSHM-CT-2006-037296 EuroIron1) to CC.

Authorship

Contribution: L.S. designed the experimental work, performed research, and cowrote the paper; A.P. performed research and analyzed data; C.C. designed research and wrote the paper.

Conflict-of-interest disclosure: The authors declare no competing financial interests.

Correspondence: Clara Camaschella, Università Vita-Salute San Raffaele, Via Olgettina, 60, 20132 Milan, Italy; e-mail: camaschella.clara@hsr.it.

References

1. Ganz T. Hepcidin, a key regulator of iron metabolism and mediator of anemia of inflammation. Blood. 2003;102:783-788.
2. Papanikolaou G, Samuels ME, Ludwig EH, et al. Mutations in HFE2 cause iron overload in chromosome 1q-linked juvenile hemochromatosis. Nat Genet. 2004;36:77-82.
3. Niederkofler V, Salie R, Arber S. Hemojuvelin is essential for dietary iron sensing, and its mutation leads to severe iron overload. J Clin Invest. 2005; 115:2180-2186.
4. Huang FW, Pinkus JL, Pinkus GS, Fleming MD, Andrews NC. A mouse model of juvenile hemochromatosis. J Clin Invest. 2005;115:2187-2191.
5. Matsunaga E, Chedotal A. Repulsive guidance molecule/neogenin: a novel ligand-receptor system playing multiple roles in neural development. Dev Growth Differ. 2004;46:481-486.
6. Matsunaga E, Nakamura H, Chedotal A. Repulsive guidance molecule plays multiple roles in neuronal differentiation and axon guidance. J Neurosci. 2006;26:6082-6088.
7. Lin L, Goldberg YP, Ganz T. Competitive regulation of hepcidin mRNA by soluble and cell-associated hemojuvelin. Blood. 2005;106:2884-2889.
8. Kuninger D, Kuns-Hashimoto R, Kuzmickas R, Rotwein P. Complex biosynthesis of the muscle-enriched iron regulator RGMc. J Cell Sci. 2006; 119:3273-3283.
9. Silvestri L, Pagani A, Fazi C, et al. Defective targeting of hemojuvelin to plasma membrane is a common pathogenetic mechanism in juvenile hemochromatosis. Blood. 2007;109:4503-4510.
10. Babitt JL, Huang FW, Wrighting DM, et al. Bone morphogenetic protein signaling by hemojuvelin regulates hepcidin expression. Nat Genet. 2006; 38:531-539.
11. Wang RH, Li C, Xu X, et al. A role of SMAD4 in iron metabolism through the positive regulation of hepcidin expression. Cell Metab. 2005;2:399-409.
12. Lin L, Valore EV, Nemeth E, Goodnough JB, Gabayan V, Ganz T. Iron transferrin regulates hepcidin synthesis in primary hepatocyte culture through hemojuvelin and BMP2/4. Blood. 2007; 110:2182-2189.
13. Babitt JL, Huang FW, Xia Y, Sidis Y, Andrews NC, Lin HY. Modulation of bone morphogenetic protein signaling in vivo regulates systemic iron balance. J Clin Invest. 2007;117:1933-1939.
14. Thompson JD, Higgins DG, Gibson TJ. CLUSTAL W: improving the sensitivity of progressive multiple sequence alignment through sequence weighting, position-specific gap penalties and weight matrix choice. Nucleic Acids Res. 1994; 22:4673-4680.
15. Lotti LV, Mottola G, Torrisi MR, Bonatti S. A different intracellular distribution of a single reporter protein is determined at steady state by KKXX or KDEL retrieval signals. J Biol Chem. 1999;274: 10413-10420.
16. Takahashi S, Nakagawa T, Kasai K, et al. A second mutant allele of furin in the processing-incompetent cell line, LoVo: evidence for involvement of the homo B domain in autocatalytic activation. J Biol Chem. 1995;270:26565-26569.
17. McMahon S, Grondin F, McDonald PP, Richard DE, Dubois CM. Hypoxia-enhanced expression of the proprotein convertase furin is mediated by hypoxia-inducible factor-1: impact on the bioactivation of proproteins. J Biol Chem. 2005;280: 6561-6569.
18. Polishchuk EV, Di Pentima A, Luini A, Polishchuk RS. Mechanism of constitutive export from the golgi: bulk flow via the formation, protrusion, and en bloc cleavage of large trans-golgi network tubular domains. Mol Biol Cell. 2003;14:4470-4485.
19. Puntervoll P, Linding R, Gemund C, et al. ELM server: a new resource for investigating short functional sites in modular eukaryotic proteins. Nucleic Acids Res. 2003;31:3625-3630.
20. Duckert P, Brunak S, Blom N. Prediction of proprotein convertase cleavage sites. Protein Eng Des Sel. 2004;17:107-112.
21. Lin L, Nemeth E, Goodnough JB, Thapa DR, Gabayan V, Ganz T. Soluble hemojuvelin is released by proprotein convertase-mediated cleavage at a conserved polybasic RNRR site. Blood Cells Mol Dis. 2008;40:122-131.
22. Hamrick SE, McQuillen PS, Jiang X, Mu D, Madan A, Ferriero DM. A role for hypoxia-inducible factor-1alpha in desferoxamine neuroprotection. Neurosci Lett. 2005;379:96-100.
23. Templeton DM, Liu Y. Genetic regulation of cell function in response to iron overload or chelation. Biochim Biophys Acta. 2003;1619:113-124.
24. Zhang AS, West AP Jr, Wyman AE, Bjorkman PJ, Enns CA. Interaction of hemojuvelin with neogenin results in iron accumulation in human embryonic kidney 293 cells. J Biol Chem. 2005;280: 33885-33894.
25. Lanzara C, Roetto A, Daraio F, et al. Spectrum of hemojuvelin gene mutations in 1q-linked juvenile hemochromatosis. Blood. 2004;103:4317-4321.
26. Zhang AS, Anderson SA, Meyers KR, Hernandez C, Eisenstein RS, Enns CA. Evidence that inhibition of hemojuvelin shedding in response to iron is mediated through neogenin. J Biol Chem. 2007;282:12547-12556.
27. Semenza GL. HIF-1 and mechanisms of hypoxia sensing. Curr Opin Cell Biol. 2001;13:167-171.
28. Ono Y, Sensui H, Sakamoto Y, Nagatomi R. Knockdown of hypoxia-inducible factor-1alpha by siRNA inhibits C2C12 myoblast differentiation. J Cell Biochem. 2006;98:642-649.
29. Wittenberg JB, Wittenberg BA. Myoglobin function reassessed. J Exp Biol. 2003;206:2011-2020.
30. Ordway GA, Garry DJ. Myoglobin: an essential hemoprotein in striated muscle. J Exp Biol. 2004; 207:3441-3446.
31. Ameln H, Gustafsson T, Sundberg CJ, et al. Physiological activation of hypoxia inducible factor-1 in human skeletal muscle. Faseb J. 2005; 19:1009-1011.
32. Lundby C, Gassmann M, Pilegaard H. Regular endurance training reduces the exercise induced HIF-1alpha and HIF-2alpha mRNA expression in human skeletal muscle in normoxic conditions. Eur J Appl Physiol. 2006;96:363-369.
33. Salvas A, Benjannet S, Reudelhuber TL, Chrétien M, Seidah NG. Evidence for proprotein convertase activity in the endoplasmic reticulum/early Golgi. FEBS Lett. 2005;579:5621-5625.
34. Le Gac G, Scotet V, Ka C, et al. The recently identified type 2A juvenile haemochromatosis gene (HJV), a second candidate modifier of the C282Y homozygous phenotype. Hum Mol Genet. 2004;13:1913-1918.
35. Peyssonnaux C, Zinkernagel AS, Schuepbach RA, et al. Regulation of iron homeostasis by the hypoxia-inducible transcription factors (HIFs). J Clin Invest. 2007;117:1926-1932.

2008 111: 924-931
doi:10.1182/blood-2007-07-100677 originally published online October 15, 2007

Furin-mediated release of soluble hemojuvelin: a new link between hypoxia and iron homeostasis

Laura Silvestri, Alessia Pagani and Clara Camaschella

Blood (print ISSN 0006-4971, online ISSN 1528-0020), is published weekly by the American Society of Hematology, 2021 L St, NW, Suite 900, Washington DC 20036.